



**HAL**  
open science

# Study of electrical malfunctions as a function of ambient temperature and carbon concentration

Marc Piller, Sylvain Suard

► **To cite this version:**

Marc Piller, Sylvain Suard. Study of electrical malfunctions as a function of ambient temperature and carbon concentration. 4th European Symposium on Fire Safety Science – ESFSS 2024, Center for Technological Risk Studies. CERTEC - Polytechnic University of Catalonia (Barcelona), Oct 2024, Barcelona, Spain. irsn-04529679

**HAL Id: irsn-04529679**

**<https://irsn.hal.science/irsn-04529679>**

Submitted on 2 Apr 2024

**HAL** is a multi-disciplinary open access archive for the deposit and dissemination of scientific research documents, whether they are published or not. The documents may come from teaching and research institutions in France or abroad, or from public or private research centers.

L'archive ouverte pluridisciplinaire **HAL**, est destinée au dépôt et à la diffusion de documents scientifiques de niveau recherche, publiés ou non, émanant des établissements d'enseignement et de recherche français ou étrangers, des laboratoires publics ou privés.

Copyright

# Study of electrical malfunctions as a function of ambient temperature and carbon concentration

Marc Piller and Sylvain Suard

Institut de Radioprotection et de Sûreté Nucléaire, PSN-RES/SA2I/LEF, Cadarache, France

## I. INTRODUCTION

As shown in the case of real fires [1], smoke can cause electrical equipment to malfunction in two ways. Firstly, the rise in ambient temperature can cause components to malfunction if the gas temperature raises the intrinsic temperature of these components beyond their critical operating temperature [2] (thermal malfunction). The soot contained in the smoke will gradually be deposited on the electronic boards; this deposition can impact the operation of the equipment in two ways: either promote the occurrence of thermal malfunction, in the event of exceeding the critical temperature of the components (the high thermal diffusivity of the soot deposition reducing the thermal inertia of the components), or generate leakage currents which disrupt the operation of the electronic boards on the surface through the formation of conductive carbon bridges [3].

This study proposes to extend the research work [4], which highlighted the effect of smoke on the malfunction of electrical equipment, in real conditions, during experimental fire scenarios in a large-scale confined installation. This study presents the results obtained on the electrical malfunction of a LOREME type electrical board, obtained using an original analytical testing device making it possible to control the exposure parameters.

## II. EXPERIMENTAL PROTOCOL

The analytical device, named DANAIDES and designed by IRSN, makes it possible to generate temperature levels from 20 to 250°C and concentrations of carbon powder regulated up to 4 g/m<sup>3</sup> around supplied electrical equipment. DANAIDES is mainly composed of an exposure chamber, an automated transfer device for the equipment tested, a closed-circuit flow circulation leg, a soot leg making it possible to achieve the concentration of interest, a ventilation turbine and a heating battery, the latter two elements being suitable for the circulation of carbonaceous aerosols (Figure 1-a). The aerosol particle generator of the DANAIDES device is the BEG 2000 generator from PALAS (Figure 1-b).

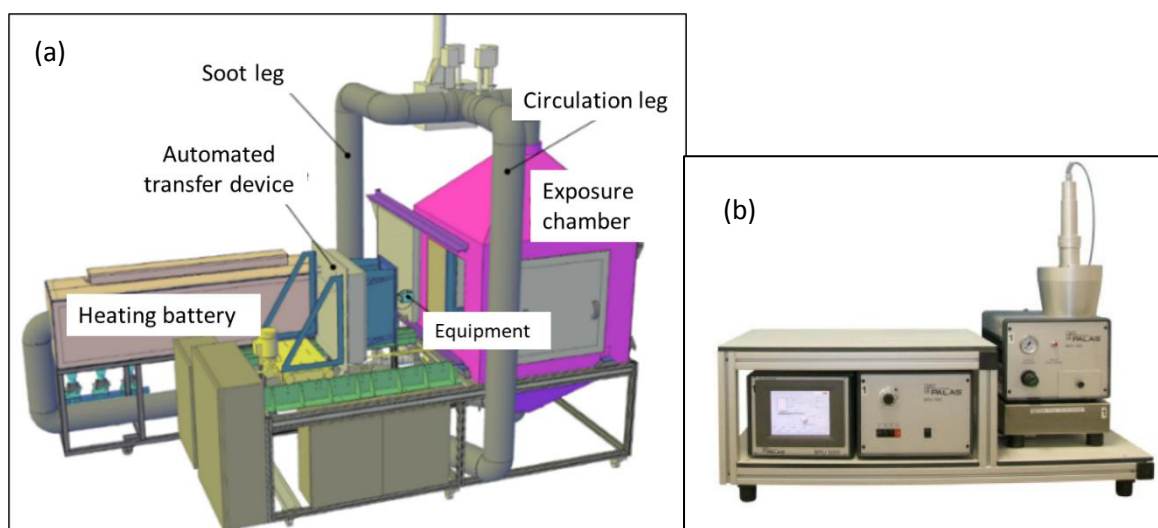
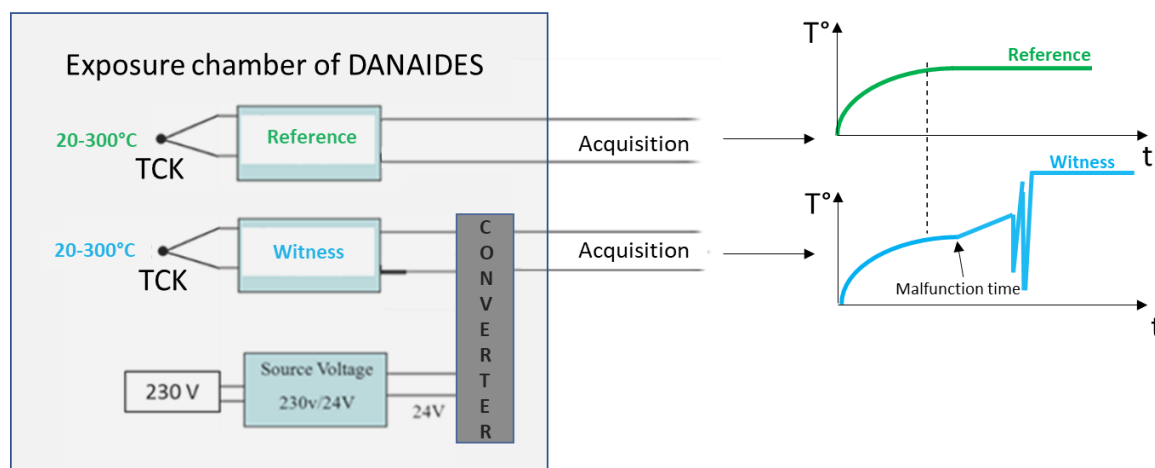


Figure 1 : DANAIDES device (a) and carbon powder particle generator (b)

The carbon powder used in DANAIDES to simulate fire soot is a glassy carbon powder, 99 % pure carbon, with a particle size of between 0.3 and 12  $\mu\text{m}$ . This particle size is representative of the average size of soot aggregates measured during large-scale fire tests, which can be well over 1  $\mu\text{m}$  [5].

The electrical equipment tested is a LOREME analog measurement converter of the CAL30iG type. For malfunction tests, the equipment was specially configured to conduct a current of intensity between 4 and 20 mA at the output, based on the signal from a type K thermocouple at the input (**Figure 2**). The tested converter is powered by 24 V DC. The converter input signal is provided by a thermocouple (the witness) measuring the temperature in the exposure chamber near the converter. The output signal, proportional to the temperature measurement of the witness thermocouple, is recorded and displayed via the acquisition/supervision system. To identify the precise moment of the converter malfunction, a second type K thermocouple is used as a reference for the temperature of the medium. This reference thermocouple is attached to the control thermocouple but does not pass through the LOREME converter tested (**Figure 2**). If the LOREME converter tested, exposed to heating and/or carbon aerosols, functions correctly, the two thermocouples (witness and reference) return the same value during acquisition, and therefore the same signal. Any deviation of the witness from the reference is therefore an indicator of a malfunction in the tested converter.



**Figure 2** : Wiring diagram of the tested equipment and identification of the malfunction moment

Carbon concentration measurements are carried out both by an on-line analyser (TEOM) during the test, as well as by sequential samples from a bank of five filters (BF), weighed after the test. Note that it is the average of the sequential samples which provides the value of the carbon concentration to be retained for the test considered (monitoring the TEOM concentration during the test makes it possible to guarantee a pseudo-stability of the level of concentration, between two BF sampling points).

### III. THERMAL MALFUNCTIONS

The first series of tests carried out in DANAIDES aims to measure the times for obtaining thermal malfunction of the equipment, under the sole effect of temperature, with a non-carbon concentration ( $C_a = 0$ ). To do this, several ambient temperature levels ( $T_a$ ) are generated around the equipment tested, and the instants of thermal malfunction, denoted  $t_T^{C_a=0}$  (index T for "Thermal"), are recorded for each value of  $T_a$ . The thermal malfunction times obtained for different ambient temperature values make it possible to construct the thermal malfunction curve without carbon powder (**Figure 3**). The regression curve of the experimental points is an inverse power law. Since the temperature rise rate of the components increases with the intensity of the initial thermal stress, it is normal that the times to obtain thermal malfunction decrease when the ambient temperature increases. Note that the first temperature to induce a thermal malfunction with zero carbon powder

concentration is 100°C (for an exposure of 30 minutes maximum); the ambient temperature at 90°C did not cause the equipment thermal malfunction.

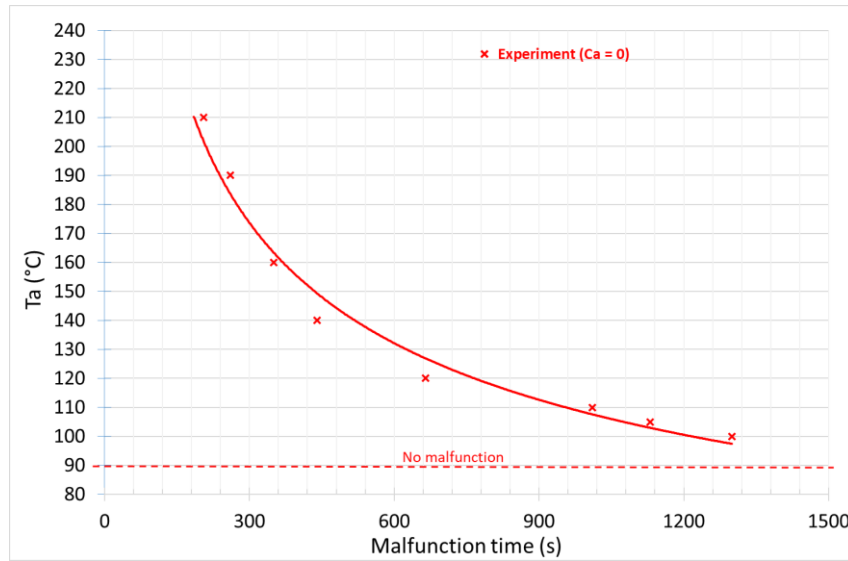


**Figure 3** : Times to obtain thermal malfunction versus ambient temperature (without carbon powder injection).

To evaluate the effect of adding carbon powder on these first thermal malfunction times, the same temperature levels (beyond 120°C to guarantee clear thermal malfunctions, whatever the concentration level of carbon powder), are generated around the equipment, but this time with a concentration  $C_a > 0$  in the flow. To do this, two concentration levels, at 2 and 3 g/m<sup>3</sup>, are regulated for each temperature series (120, 140, 160, 190 and 210°C). Thermal malfunction times in the presence of carbon powder denoted ( $t_T^{C_a}$ ), are reported in **Figure 4** with the associated trend lines.

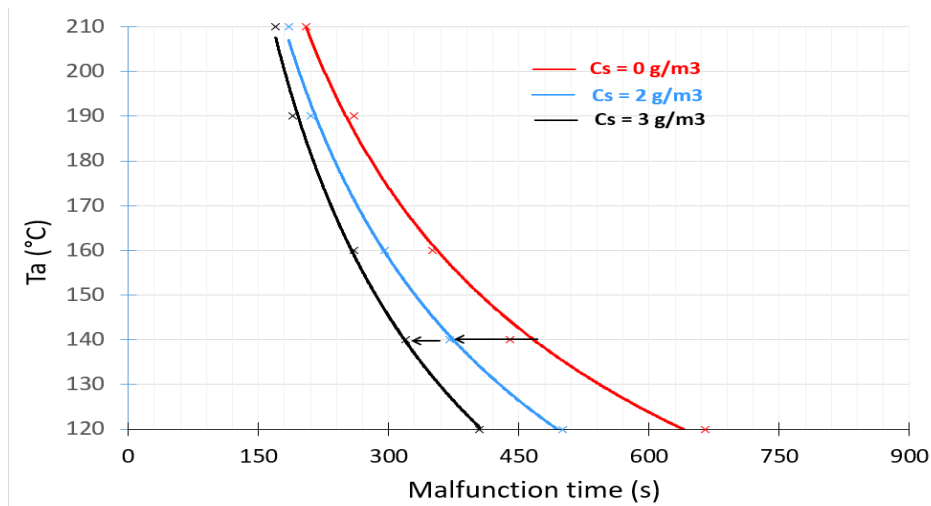


**Figure 4** : Reduction of times to obtain thermal malfunction by different carbon concentration values.

In **Figure 4**, irrespective of the carbon concentration, the times to obtain thermal malfunction decrease with ambient temperature (decreasing power law). For a set temperature, the greater the concentration of carbon powder in the flow, the shorter the time for the thermal malfunction to appear. In order to explain how carbon aerosols shorten the thermal malfunction times for the same ambient temperature, **Figure 5** first shows the temperature rise curves measured inside the equipment (using a through thermocouple in contact with the electronic board), without carbon injection (0 g/m<sup>3</sup>) and with a carbon concentration regulated to 3 g/m<sup>3</sup>, for two different ambient temperature exposures (160° C and 190°C).

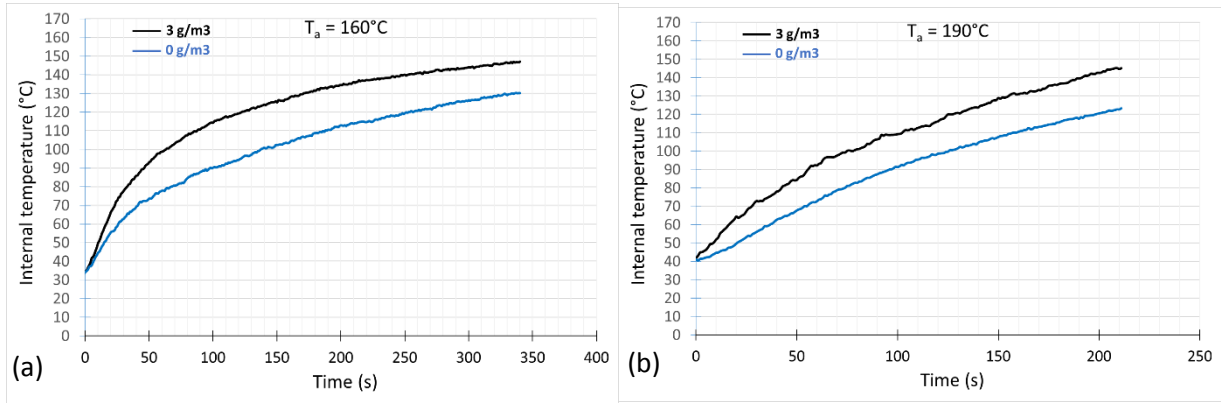


**Figure 5** : Impact of carbon concentration on the change in the internal temperature of the equipment for two ambient temperatures: a)  $T_a = 160^\circ\text{C}$ , b)  $T_a = 190^\circ\text{C}$

In **Figure 5**, regardless of the exposure temperature (160 or  $190^\circ\text{C}$ ), the temperature rise rate of the internal electronic board increases when carbon particles are added to the hot air flow. To understand this phenomenon, let's use the thermal properties of carbon (the carbon particles used are 99% pure carbon particles).

For carbon, taking the usual data from the literature:  $\lambda = 155 \text{ W m}^{-1}\text{K}^{-1}$ ,  $\rho = 2000 \text{ kg.cm}^{-3}$ , and  $C_p = 709 \text{ JK}^{-1}\text{kg}^{-1}$ , the thermal diffusivity  $a$  is equal to  $109 \mu\text{m}^2/\text{s}$ . This diffusivity value is in the high range of materials, at the same level as most conductive metals (ranging between 10 and  $130 \mu\text{m}^2/\text{s}$ ). This value is well above the diffusivity range of plastics (generally less than  $1 \mu\text{m}^2/\text{s}$ ), and even higher if we compare it with those of Epoxy resins (which cover most electronic components), around  $0.1 \mu\text{m}^2/\text{s}$ . So on the basis of this very high thermal diffusivity, the carbon spherules injected into the flow will quickly reach the exposure temperature, well before the electronic components exposed to the same temperature level. The layer of hot carbon particles, which gradually forms on the internal surfaces of the equipment, will therefore heat the components by conduction, more efficiently (and therefore more quickly) than when they are only subjected to convective flows exchanged with hot air.

## IV. MALFUNCTIONS DUE TO LEAKAGE CURRENTS

### IV.1 Results

Following the characterization of the thermal malfunction times of the components (effect of air temperature combined with the thermal properties of the carbon powder), the study now aims to characterize the malfunction times obtained by electrical disturbances linked to leakage currents passing through carbon bridges formed by carbon deposition (short circuits between components normally isolated from each other). To isolate this type of malfunction, it will be studied at temperatures remaining below the thermal malfunction threshold (i.e.  $\leq 90^\circ\text{C}$ , as shown in **Figure 3**).

In this part, three levels of carbon concentration ( $C_a = 1, 2$  and  $3 \text{ g/m}^3$ ) are regulated around the equipment with, for each of these levels, four levels of ambient temperature:  $T_a = 20, 55, 80$  and  $95^\circ\text{C}$ . The associated malfunction curves, namely the times to obtain the leak malfunction, denoted  $t_L^{T_a}$  (index L for "Leakage"), are plotted in **Figure 6** versus concentration  $C_a$  and ambient temperature  $T_a$ . The regression curves of the experimental points follow an increasing logarithmic law.

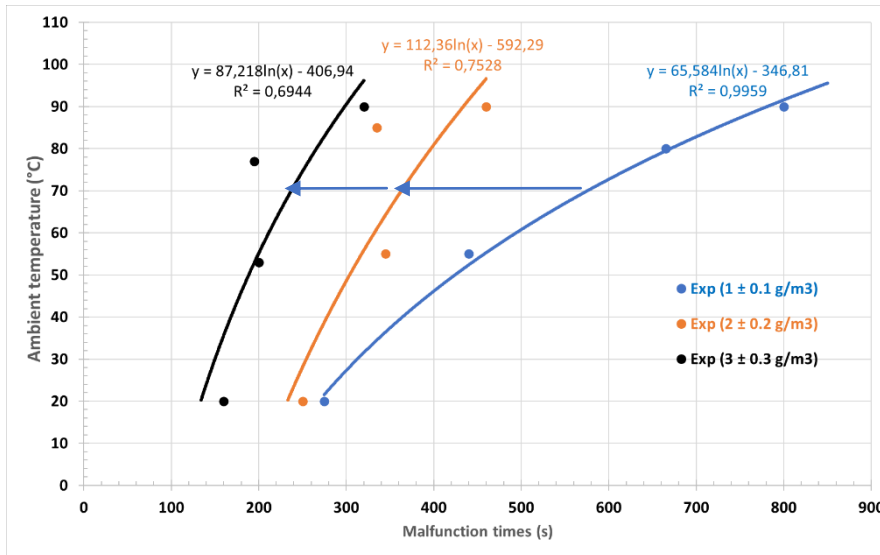


**Figure 6 :** Effect of carbon concentration on leak malfunction times, for different exposure temperatures (below the minimum thermal malfunction temperature).

As with thermal malfunctions, leak malfunction times at a set temperature are shortened as the carbon concentration increases (**Figure 6**). This is consistent when it is considered that the greater the quantity of carbon available, the more quickly critical deposition is reached (allowing for leakage currents). On the other hand, unlike thermal malfunctions, it is observed that at a set carbon concentration, the times to obtain leak malfunctions increase with ambient temperature.

#### IV.2 Analysis and explanation of leak malfunction times increasing with temperature.

The carbon deposits obtained for three LOREME equipment items, tested with an identical carbon concentration ( $2 \text{ g/m}^3$ ), different exposure durations and different ambient temperatures, were photographed (**Figure 7-a**) under a high magnification optical microscope (MOD), in the same area on the electronic board (green square, **Figure 7-b**). The three equipment items underwent the following history: (I) exposure to  $90^\circ\text{C}$  until the malfunction (leak) time, i.e. for 460 s; (II) exposure to  $20^\circ\text{C}$  until malfunction (leak) time, i.e. for 250 s; and (III) exposure to  $90^\circ\text{C}$  limited to 250 seconds of exposure duration (the same duration as for  $20^\circ\text{C}$ ) not causing the equipment malfunction.

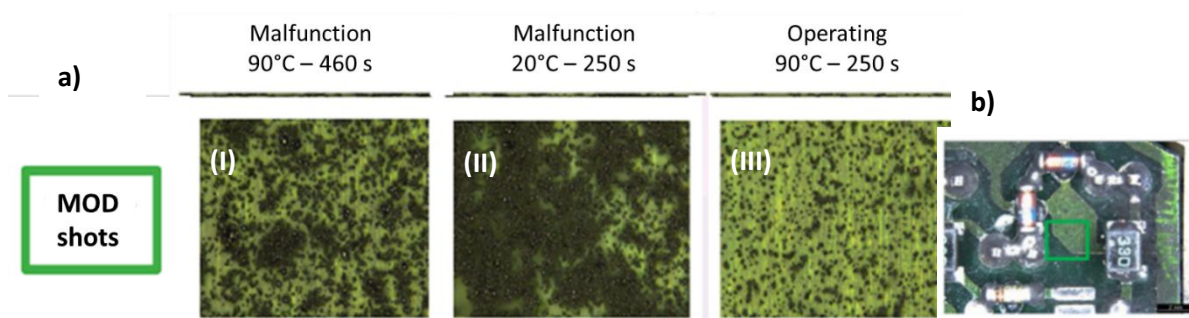


**Figure 7 :** (a) Photographs (MOD) of the carbon deposit (black points) on the electronic boards (green surfaces) for three equipment items exposed to  $2 \text{ g/m}^3$  of carbon powder: (I)  $90^\circ\text{C}$  / 460s (malfunction time), (II)  $20^\circ\text{C}$  / 250s (malfunction time), (III)  $90^\circ\text{C}$  / 250s (operating). (b) Photographed zone for the three equipment items.

Photos (II) and (III) in **Figure 7** show that after the same exposure time (250 s) and the same aerosol concentration ( $2 \text{ g/m}^3$ ), the carbon coverage is significantly stronger for the equipment tested at  $20^\circ\text{C}$  than for that at  $90^\circ\text{C}$ . This observation is confirmed by the mass measurements deposited on the equipment after testing: 292 mg at  $20^\circ\text{C}$  compared to 154 mg at  $90^\circ\text{C}$ , for the same exposure time (250 s). To explain why the deposit decreases at higher temperatures, we can refer to studies on the

flowability of powders showing that the cohesion of the powders is linked to the intensity of the internal forces present such as the Van der Waals forces or the capillary forces (liquid bridges) between particles [6][7]. Considering that as the air temperature increases, the carbon powder dries out during transport, thereby reducing capillary forces, we understand why flowability increases with a dry powder [8]. At a set carbon concentration, the loss of powder adhesion with temperature therefore reduces the rate of carbon deposition, and ultimately delays the formation of the cohesive carbon bridges causing the leakage currents between components.

Another observation can be made by comparing images (I) and (II). On these two photos, showing equipment items which both malfunctioned at the end of the exposure, the critical deposition density appears less dense at 90 °C than at 20 °C. It would therefore seem that the increase in temperature makes it possible to generate leakage currents with less deposition. Without being able to demonstrate it experimentally at this stage, one way of demonstrating this phenomenon could be found in the electrical properties of carbon, which normally has an electrical resistivity which decreases with temperature. [9].

**V. SYNTHESIS OF MALFUNCTIONS DEPENDING ON THE AMBIENT TEMPERATURES.**

The synthesis of all the malfunctions obtained from 20 to 210 °C, in **Figure 8**, is achieved by compiling the results presented in **Figure 4** and **Figure 6**. On this new graph, we slightly extend (dotted line) the two types of curves (inverse power law for thermal malfunction times and increasing logarithmic law for leakage currents), and they come together around certain temperatures: 115 °C at 2 g/m<sup>3</sup> and 120 °C at 3 g/m<sup>3</sup>. The straight line (dotted, in **Figure 8**) passing through these convergence temperatures then separates the two distinct zones of malfunction versus the ambient temperature and the carbon concentration: thermal malfunctions (the components reach the critical temperature, above the line) and malfunctions of leakage currents (below the line, the critical temperature is never reached before the carbon bridges). This straight line is called the mode transition line. Note that the minimum temperatures allowing thermal malfunction (on the dotted line) increase with the carbon concentration present (about 100 °C without carbon injection, approximately 115 °C with 2 g/m<sup>3</sup> and 120 °C with 3 g/m<sup>3</sup>). This increase of the transition ambient temperatures with carbon concentration is logical, since the more the carbon concentration increases, the faster the formation of carbon bridges becomes, and so the higher the ambient temperature must be to reach the component critical temperature before leakage currents are created.

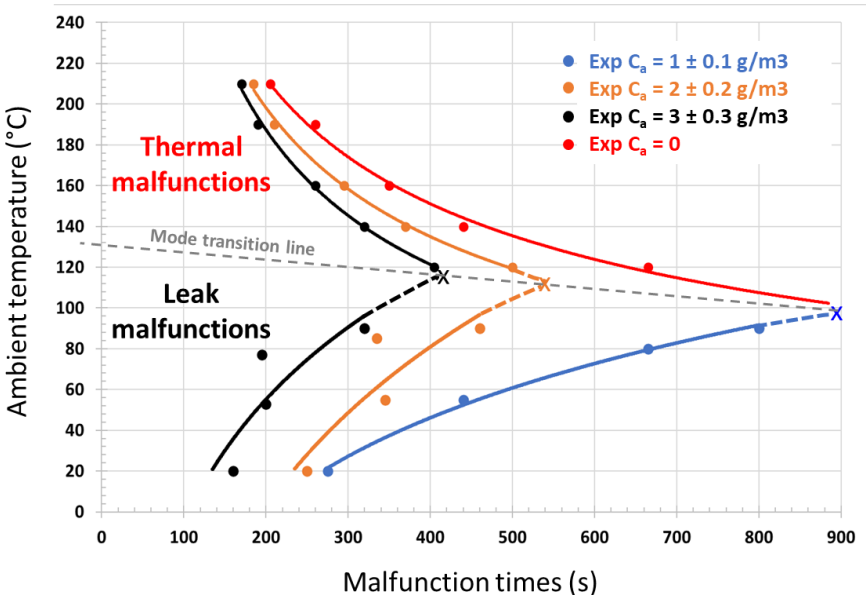


**Figure 8** : Synthesis of both thermal and leak malfunction times versus ambient temperature and carbon concentration.



## VI. CONCLUSION

This study has demonstrated that the addition of carbon particles to the flow always promotes the occurrence of electrical malfunctions, regardless of the ambient temperature. For temperatures above 120 °C, i.e. located above the mode transition line (with a maximum concentration equal to 3 g/m<sup>3</sup> of carbonaceous aerosols), the carbon powder which is deposited on the equipment has the effect of heating components faster up to their critical temperature, due to the high thermal diffusivity of carbon. At temperatures where thermal failure of components is no longer possible before the formation of conductive carbon bridges (i.e. below the mode transition line), critical carbon deposition then causes malfunctions through leakage current generation. In the latter case, it was observed that for the same carbon concentration, the leak malfunction onset times increase with ambient temperature, due to the reduction in the adhesion forces of the carbon powder (through temperature-dependent drying).

## References

- [1] DOE Handbook, Fire effects on Electrical and Electronic Equipment, Fire Protection Volume II, Chapter 2.0, Background, DOE-HDBK-1062.96, August 1996
- [2] DOE Handbook, Fire effects on Electrical and Electronic Equipment, Fire Protection Volume II, Chapter 3, Effect of heat on electronic equipment (p.40), DOE-HDBK-1062.96, August 1996
- [3] T.J. Tanaka, S. Nowlen, D.J. Anderson, "Circuit bridging of Components by smoke" NUREG/CR-6476 SAND96-2633, 1996
- [4] M. Piller, M. Coutin, "Effects of smoke and thermal stress on electrical equipment failures", 15th SMIRT Post-conference seminar on fire safety in nuclear power plants and installations, Bruges, Belgium, October 4-5, 2017
- [5] F.X Ouf, V.-M. Mocho, S. Pontreau, Z. Wang, D. Ferry and J. Yon, Clogging of Industrial High Efficiency Particulate Air (HEPA) Filters in Case of Fire: From Analytical to Large-Scale Experiments, *Aerosol Science and Technology*, 48:939–947, 2014.
- [6] J. Tea. Evaluation de la coulabilité des poudres, Comparaison de méthodes de mesure, *Sciences pharmaceutiques*, 2015. ffhal-01732354
- [7] U. Zafar et al., A review of bulk powder caking. *Powder Technology* 313 (2017) 389–401. <http://dx.doi.org/10.1016/j.powtec.2017.02.024>
- [8] D. Yamaguchi, Powder properties of carbon-based solid acid catalyst for designing cellulose hydrolysis reactor with stirring apparatus. *Heliyon* 9 (2023) e21805. <https://doi.org/10.1016/j.heliyon.2023.e21805>
- [9] R.E. Taylor, H. Groot, Thermophysical Properties of POCO Graphite, (West Lafayette, Indiana: Purdue University, July 1978 [NTIS No. ADA060419])